Numerical Investigation of Fluid Flow and Heat Transfer characteristics in cooling of Electrical Motor by Using Nanofluid in the Spiral Channel

Ali Deriszadeh[1], Filippo de Monte[1]

[1] *Department of Industrial and Information Engineering and Economics, University of L'Aquila, L'Aquila, Italy*
Corresponding author e-mail: ali.deriszadeh@graduate.univaq.it

Abstract. In this paper, properties of flow and heat transfer of nanofluid in the spiral channel used in the cooling system of an electric motor are numerically investigated. The finite element method is used to solve the governing equations. The flow regime is considered as laminar and the base fluid is water. In addition to pure water flow, the effect of adding Aluminium-Oxide nanoparticles in the base fluid on the heat transfer performance of the cooling system is studied. The Reynolds number of the fluid, turns number of the spiral channel, volume fraction of the nanofluid, and pressure drop of the coolant are the most important evaluation parameters of this study. Heat transfer analyses are performed based on computational fluid dynamics and 3D fluid motion analysis.

1. Introduction

Energy conversion process in electric motors generates heat flux and increases the temperature. The function of electric motor can be influenced by this increase in temperature. Reducing the operating temperature will increase the efficiency and the lifetime of the electric machine. Therefore, the cooling of electric motors, which sometimes their temperature increases up to 180 ° C, has always been of particular importance. Generated heat in electric motors is because of ohmic losses of windings (Joule losses), iron losses, mechanical losses, and stray load losses [1].

Air or water are the most commonly used cooling fluids in the cooling system of electrical motors. In order to increase the heat transfer, fins attached to the body of electric motor are also used, which in some cases is not practical due to space constraints. In case a fluid is used for cooling, the temperature of the electric motor can be reduced by increasing the heat transfer coefficient of the coolant. In [2], an empirical investigation of an enclosed cooling system for electric motor has been performed.

Cooling jackets are among the coolant methods of electric motors in which the cooling fluid absorbs the heat flux generated by the electric motor and causes the engine to cool down. Increasing the thermal capacity of the coolant fluid and increasing the speed of the coolant fluid are methods for improving heat transfer of a cooling system [3-4]. Vortex generators are also used in the cooling jacket to increase heat transfer capability of the cooling system. Vortex generators increase the heat transfer coefficient by changing the fluid velocity profile, changing boundary layer arrangements, and by generating the secondary flow. In [5] – [9], the use of the winglet vortex generator, triangular barrier, and rib-roughened channels were investigated.

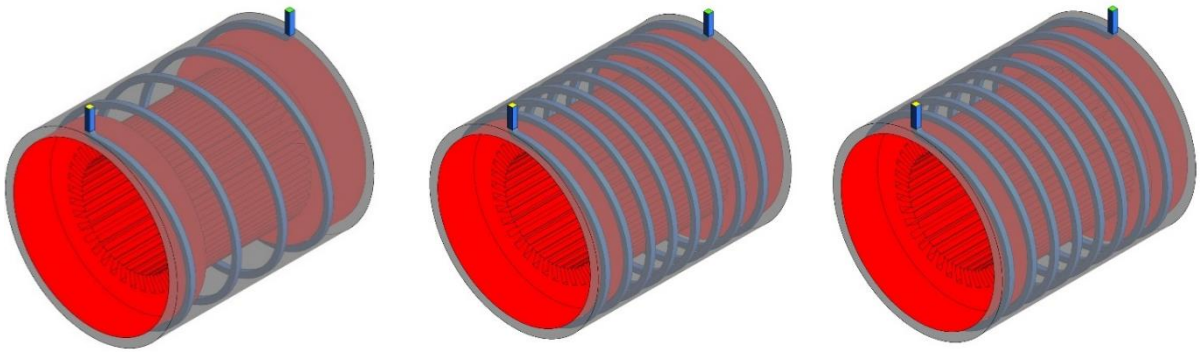

(a) (b) (c)

Figure 1. schematic of the cooling system with (a) 4 turns, (b) 6 turns, and (c) 8 turns.

In designing of electric motor cooling jackets, the exact prediction of thermal behaviour is an inevitable need. In [10]-[15], temperature analyses of fan-cooled machines have been investigated in order to properly understand the heat transfer of electric motor and to identify the effective parameters on achieving high efficiency and optimal robust design.

In the designing of the cooling system, it must be ensured that the maximum temperature does not reach maximum allowed temperature of the electric motor. In [16], performance of a half-coiled jacket with delta winglet vortex generator was examined. Results show that the heat transfer is unpredictable in the case where the angle of the delta winglet is 25 to 30 degrees.

Recently, usage of nanoparticles in coolant fluids has attracted much attention of researchers due to its advantage of increasing heat transfer capability of cooling system [17]. Nanoparticles, due to their high thermal conductivity coefficients, increase the heat transfer rate and improve the performance of the cooling system [18].

It is worthwhile noting that, although using nanofluid coolants leads to the increase in heat transfer capability of the coolant, due to the increase in the density and viscosity of the fluid because of the addition of nanoparticles, the pressure drops and required pumping power in the fluid increase. This is not a desirable fluid phenomenon. Therefore, for cooling systems employing nanofluid coolants, both thermal and fluid performance analyses are necessary [19]. In [20], the effect of vortex generators and aluminium-oxide nanoparticles in the water base fluid was investigated and compared to pure water coolant. It was concluded that the use of nanofluid and vortex generates improve heat transfer capability of the cooling system up to 2.7 times than using pure water coolant.

In this paper, the thermal performance of indirect cooling system of electric motor using cooling jacket and nanofluid coolant is investigated using finite element method. First, effect of turns number of spiral pipes and the flow rate (Reynolds number) of the coolant on heat transfer performance of the cooling system are investigated; then, in the case of maximum obtained heat transfer, the effect of employing Aluminium-oxide nanoparticles in the base fluid is studied.

2. Problem and Boundary Conditions

The designed cooling system in this paper consists of a cooling jacket with spiral cooling channels. Fig 1 shows schematic of the cooling system. Cooling channels carrying nanofluid are made of Aluminium and material of electric motor body is steel. The applied boundary conditions are shown in Fig 2. As can be seen, boundary conditions are the inlet velocity of fluid with temperature of 343 K and the outlet pressure. Stator and its cooling jacket are under heat flux of 3500 W/m2. The wall where the channels are inside it is considered as insulated.

To improve heat transfer of the cooling system, Aluminium-oxide nanoparticles are added to the base fluid. Effects of adding nanoparticles on flow and thermal performance of the cooling system are studied for three different volume fractions of the nanofluid.

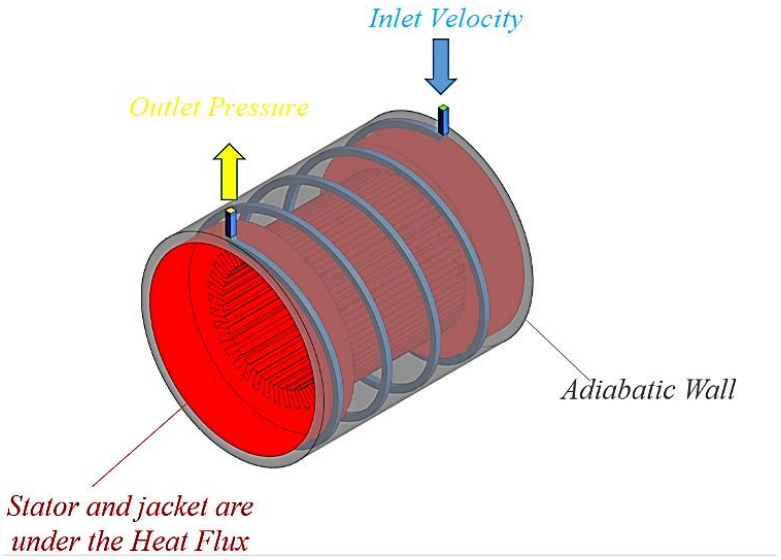

Figure 2. Applied boundary conditions.

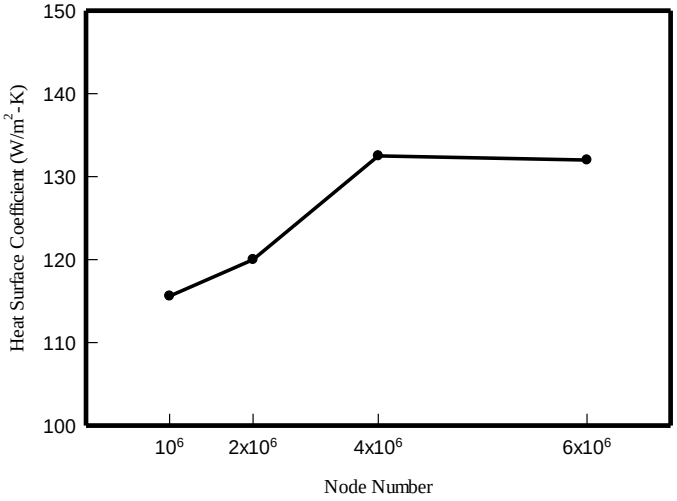

Figure 3. Calculated heat transfer coefficient versus number of nodes.

The number of nodes in the meshed model has a significant effect on the accuracy of obtained numerical results. To investigate the effect of number of mesh nodes on the accuracy of obtained numerical results, different simulations were performed and the heat transfer coefficient versus number of nodes is presented in Fig 3. As can be seen, as the number of nodes exceeds 6 × 104, the heat transfer coefficient does not change. Therefore, 6 × 104 nodes are considered in the simulations. Due to density of meshes, a computer server with 48 cores and 124GB of RAM is used.

3. Governing equations

Governing equations in the Cartesian coordinates and in steady state are as follows [21].

3.1. conjugation equation

Conjugation equation is given as:

$$\frac{\partial(u)}{\partial x} + \frac{\partial(v)}{\partial y} + \frac{\partial(w)}{\partial z} = 0 \tag{1}$$

where *u, v, and w* are fluid velocities along *x*-, *y*-, and *z*-axis, respectively.

3.2. Momentum equation

The Momentum equation in x-axis direction is as follows.

$$u\frac{\partial(u)}{\partial x}+v\frac{\partial(u)}{\partial y}+w\frac{\partial(u)}{\partial z}=-\frac{1}{\rho_{nf}}\frac{\partial P}{\partial x}+\nu_{nf}\left(\frac{\partial}{\partial x}\left(\frac{\partial u}{\partial x}\right)+\frac{\partial}{\partial y}\left(\frac{\partial u}{\partial y}\right)+\frac{\partial}{\partial z}\left(\frac{\partial u}{\partial z}\right)\right) \quad (2)$$

where ρ_{nf} is density of nanofluid and p is pressure. ν_{nf} is coefficient of Kinematic viscosity.

The Momentum equation in y-axis direction:

$$u\frac{\partial(v)}{\partial x}+v\frac{\partial(v)}{\partial y}+w\frac{\partial(v)}{\partial z}=-\frac{1}{\rho_{nf}}\frac{\partial P}{\partial x}+\nu_{nf}\left(\left(\frac{\partial}{\partial x}\left(\frac{\partial v}{\partial x}\right)+\frac{\partial}{\partial y}\left(\frac{\partial v}{\partial y}\right)+\frac{\partial}{\partial z}\left(\frac{\partial v}{\partial z}\right)\right)\right) \quad (3)$$

The Momentum equation in z-axis direction:

$$u\frac{\partial(w)}{\partial x}+v\frac{\partial(w)}{\partial y}+w\frac{\partial(w)}{\partial z}=-\frac{1}{\rho_{nf}}\frac{\partial P}{\partial x}+\nu_{nf}\left(\frac{\partial}{\partial x}\left(\frac{\partial w}{\partial x}\right)+\frac{\partial}{\partial y}\left(\frac{\partial w}{\partial y}\right)+\frac{\partial}{\partial z}\left(\frac{\partial w}{\partial z}\right)\right) \quad (4)$$

3.3. Energy equation:

$$u\frac{\partial(T)}{\partial x}+v\frac{\partial(T)}{\partial y}+w\frac{\partial(T)}{\partial z}=\alpha_{nf}\left(\frac{\partial}{\partial x}\left(\frac{\partial T}{\partial x}\right)+\frac{\partial}{\partial y}\left(\frac{\partial T}{\partial y}\right)+\frac{\partial}{\partial z}\left(\frac{\partial T}{\partial z}\right)\right) \quad (5)$$

where α_{nf} is thermal diffusivity of the nanofluid and T is temperature.

3.4. The governing equations for calculating the properties of nanoparticles and calculated parameters

Determination of thermophysical properties to discover flow behaviour and heat transfer at different volume fractions of nanofluid are implemented by using valid empirical relationships for parameters such as density, specific heat capacity, thermal conductivity coefficient and Nanofluid viscosity are given as follows.

$$\rho_{nf}=(1-\varphi)\rho_f+\varphi\rho_p \quad (6)$$

$$\left(\rho C_p\right)_{nf}=(1-\varphi)\left(\rho C_p\right)_f+\varphi\left(\rho C_p\right)_p \quad (7)$$

$$\frac{k_{eff}}{k_f}=\frac{k_p+2k_f+2\varphi\left(k_p-k_f\right)}{k_p+2k_f-\varphi\left(k_p-k_f\right)} \quad (8)$$

$$\mu_{nf}=\mu_f(123\varphi^2+7.3\varphi+1) \quad (9)$$

where φ, ρ_f, and ρ_p are volume fraction of nanofluid, density of fluid, and density of nanoparticles, respectively. Cp is specific heat capacity and K is thermal conductivity. K_{eff} is effective thermal conductivity. μ_{nf} and μ_f are coefficient of dynamic viscosity of nanofluid and fluid, respectively.
In calculation of the Reynolds number, the channel inlet diameter and nanofluid properties are used as follows.

$$Re=\frac{\rho_{nf}u_{in}D}{\mu_{nf}} \quad (10)$$

In (10), u_{in} is fluid inlet velocity and D is hydraulic diameter.

Fluid displacement heat transfer coefficient is expressed as follows.

$$h=\frac{q_w}{(T_w-T_b)} \quad (11)$$

Table 1. Characteristics of Aluminum-oxide nanoparticles for different volume fractions [22].

φ(%)	ρ (J/kg K)	C_p (kg/m^3)	k (W/m K)
0 φ=	998.2	4182	0.613
0.02 φ=	1056.6	3922.4	0.6691
0.04 φ=	1116	3693.2	0.7296
Al_2O_3	3970	765	40

where h is heat transfer coefficient. T_w and T_b are wall and bulk temperatures, respectively. q_w is wall heat flux.

To calculate the Nusselt number, the following equation is used.

$$Nu = \frac{h \cdot D}{k_{nf}} \tag{12}$$

To calculate the Nusselt number, the following equation is used.

$$Nu = \frac{hD}{k_{nf}} \tag{12}$$

To evaluate the overall thermal and fluid performance of the cooling system, an evaluation parameter (PEC) is defined as follows.

$$PEC = \frac{\left(\frac{Nu_{ave}}{Nu_{ave,s}}\right)}{\left(\frac{f}{f_s}\right)^{(1/3)}} \tag{13}$$

where, $N_{uave,s}$ and f_s are base parameters and are defined for the base fluid (pure water). Indeed, PEC indicates the ratio of the increase in heat transfer and the increase in the pressure drop of the nanofluid in comparison with the base fluid.

According to empirically validated relationships, thermophysical properties of solid Aluminum-oxide nanoparticles [22] and Aluminum-oxide-Water nanofluid such as density, thermal capacity, thermal conductivity coefficient, and dynamic viscosity for different volume fractions of the solid nanoparticles are listed in Table 1.

4. Results

In order to investigate the effect of cooling channels turns number on heat transfer performance of the cooling system, the average temperature of motor in terms of Reynolds number at different turns numbers is shown in Fig 4. According to Fig 4, for all the turn numbers, under a constant heat flux, as the Reynolds number increases, the average temperature of the channels' wall decreases. For example, the cooling system with 8 turns number at Reynolds number of 500, the average temperature of the channels' wall is 387 K and at Reynolds number of 2000, the average temperature is 377 K; which shows that with 4 times increase of the flow rate of the fluid passing through the 8 turns spiral channels, the average temperature has decreased by 10 K. Improvement of the heat transfer is because of the increased heat absorption capacity due to the increase of the flow rate of the coolant fluid. This leads to a more heat flux absorbed by the fluid and the fluid temperature is lowered.

Investigating the effect of turns number of cooling channels on heat transfer performance of the cooling system under a constant Reynolds number indicates that by increasing the turns number, due to the increase in the cooling cross-sectional area, the heat transfer from the motor to the coolant fluid increases. Therefore, the average wall temperature decreases. For example, the fluid with Reynolds number of 2000, in turns number of 8, 6, and 4, the average wall temperature of channels is 377 K, 380 K, and 386 K, respectively.

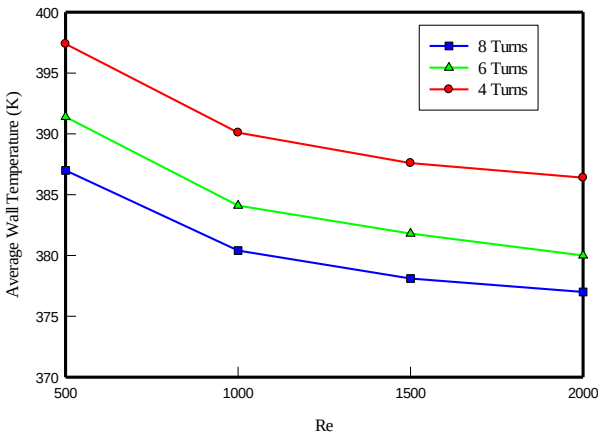

Figure 4. Average temperature of motor in terms of Reynolds number at different turns numbers.

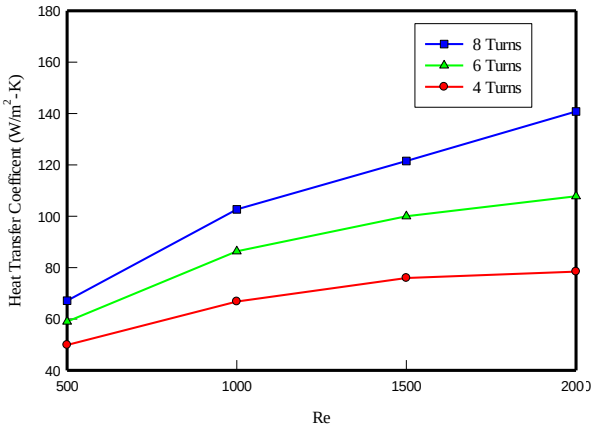

Figure 5. Effect of Reynolds number and turns number on heat transfer performance of the cooling system.

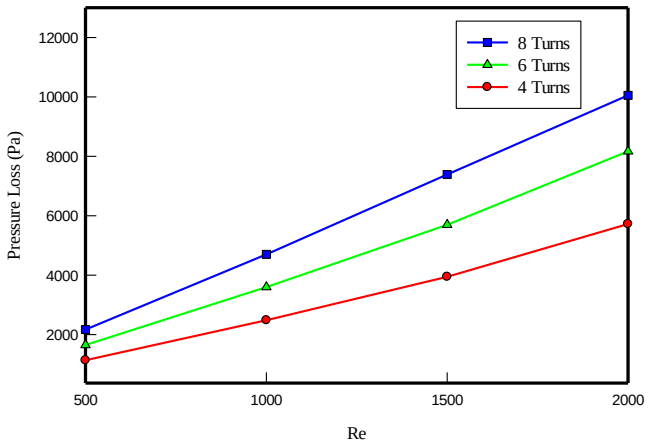

Figure 6. Pressure drop versus the Reynolds number for three different turns numbers.

For further investigation of the effect of Reynolds number and turns number on heat transfer performance of the cooling system, the heat transfer coefficient in terms of three different Reynolds numbers is shown in Fig 5. As can be seen in Fig 5, with the increase of the Reynolds number, heat transfer coefficient increases. This is due to an increase in temperature difference between channels walls and fluid resulted from increase in fluid flow and an increase in the heat absorption capacity of the flowing wall. As mentioned above, at 8 turns, the increase of the Reynolds number from 500 to 2000 decreases the wall temperature by 10 degrees. The heat transfer coefficient analysis also shows that with increase of the Reynolds number from 500 to 2000, the heat transfer coefficient increases from 67 to 140 W/m^2-k.

In addition to checking the cooling performance of the system, it is necessary to examine its properties from the fluid dynamic perspective too. For this purpose, the pressure drop in terms of the Reynolds number in three different turns numbers is shown in Fig 6. As can be seen, at constant Reynolds number, the pressure drop increases with increasing of the turns number. The increase in the pressure drop is due to changes of the flow path of the fluid, the increase in turns number, changes of the velocity gradient, and the change of the arrangement of the boundary layer, cause the drop in fluid pressure. By increase of the Reynolds number at constant turns number, as expected, the pressure drop has also been increased. The increase of pressure drop by increasing the Reynolds number leads to more power needed for pumping the increased inlet fluid flow.

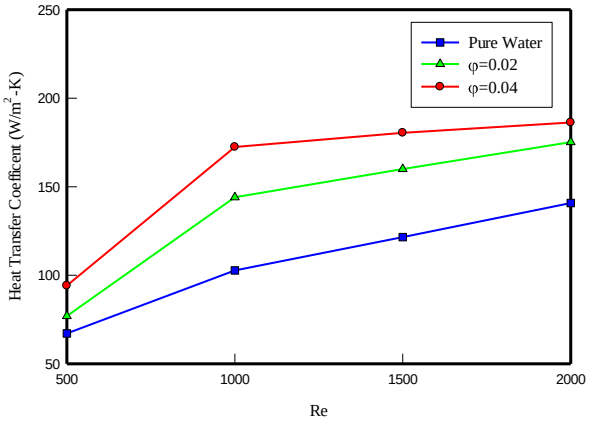

Figure 7. The effect of nanoparticles volume fraction on increasing of heat transfer.

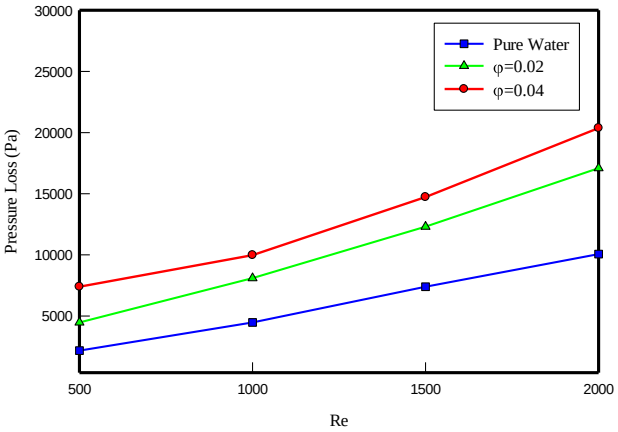

Figure 8. The effect of nanoparticles volume fraction on increasing of pressure drop.

Heat transfers of nanofluids with volume fractions of 2% and 4% are shown in Fig 7. As can be seen, by increasing the volume fraction of nanoparticles in the fluid, the heat transfer from channel's walls to the cooling fluid increases and the motor temperature decreases. The improvement in cooling due to the use of nanoparticles in the base fluid results from the fact that the addition of nanoparticles to the base fluid increases its conduction heat transfer coefficient. This improves thermal penetration depth of the coolant fluid. Also, the presence of a nanoparticle in the base fluid leads to a reduction in specific heat capacity of the base fluid. This increases amount of the absorbed heat flux by the coolant fluid. These two factors reduce the operating temperature of the motor and improve heat transfer performance of the cooling system. Fig 8 shows increase of pressure drop caused by increase of Reynold number and volume fraction of nanoparticles.

5. Conclusion

Using a 3D Finite element method, a cooling system of an electric motor has been simulated in this paper. To increase the heat transfer capability of the cooling system and to reduce operating temperature of the electric motor, a nanoparticle of Aluminium-oxide has been added to the base fluid (pure water). The effect of nanoparticle volume fraction on the flow and heat transfer properties of the nanofluid coolant has been investigated. Also, the effect of the flow rate of the cooling fluid and turns number of spiral channels on heat transfer capability of the cooling system have been studied. The studied results include heat transfer coefficient, pressure drop and average temperature. The numerical results show that with increasing Reynolds number, the operating temperature of the electric motor decreases and the pressure drop increases. According to the simulation results, adding nanoparticles with volume fraction of 4%, increases the heat transfer capability of the cooling system up to 40%. The performance coefficient test shows that the increase in the pressure drop due to the addition of nanoparticles in fluids with a low Reynolds number (500) is significand while increase in heat transfer capability is very limited. Also, in Reynolds number of 2000, addition of nanoparticles with volume fraction of 2% and 4% almost lead to a same performance. Therefore, it can be concluded that by considering thermal and fluid performance of the system with Reynolds number of 2000, the use of Aluminium-oxide nanoparticle with 2% volume fraction shows better heat transfer performance and is more cost-effective. Finally, according to the results, in case of using fluid with Reynolds number of 1000 for both volumetric 2% and 4% and with channel turns number of 8, improvement in heat transfer capability is more remarkable compare to the increase of pressure drop.

6. References

[1] Huai Y, Melnik R.V.N, Thogersen P.B 2003 Computational analysis of temperature rise phenomena in electric induction motors, *Appl. Therm.* pp 779– 795.

[2] Farsane K, Desevaux P, Panday P.K 2000 Experimental study of the cooling of a closed type electric motor, *Appl. Therm.* pp 1321–1334.

[3] Henneberger, G, Yahia K.B, Schmitz M 1995 Calculation and identification of a thermal equivalent circuit of a water-cooled induction motor for electric vehicle applications. *the Seventh International Conference on Electrical Machines and Drives*.

[4] Haumer C, Bauml A, Thermal T 2008 model and behavior of a totally-enclosed-water-cooled squirrel-cage induction machine for traction applications. *IEEE Trans. Ind. Electron*. pp 3555–3565.

[5] Cengiz Y, Yasar B, Dursun P 1997 Heat transfer and pressure drops in a heat exchanger with a helical pipe containing inside springs, *Energy Convers. Manage*, pp 619–624.

[6] Zachár A 2010 Analysis of coiled-tube heat exchangers to improve heat transfer rate with spirally corrugated wall, *Int. J. Heat Mass Transf*. pp 3928–3939.

[7] Biswas G, Torii K, Fujii D, Nishino K 1996 Numerical and experimental determination of flow structure and heat transfer effects of longitudinal vortices in a channel flow, *Int. J. Heat Mass Transf.* pp 3441–3451.

[8] Biswas G, Chattopadhyay H, Sinha A 2012 Augmentation of heat transfer by creation of streamwise longitudinal vortices using vortex generators, *Heat Transf.* pp 406–424.

[9] Mitra N.K, Fiebig M 1994 Comparison of wing-type vortex generators for heat transfer enhancement in channel flows, *J. Heat Transf*, pp 880–885.

[10] Bauml, T, Kral, C, Haumer, A, Kapeller H 2007 Enhanced thermal model of a totally enclosed fan cooled squirrel cage induction machine. *IEEE International Electric Machines & Drives Conference,* pp. 1054–1058.

[11] Du Y, Thomas G. Habetler, Ronald Gordon Harley 2008 Methods for thermal protection of medium voltage induction motors — A review, International Conference on Condition Monitoring and Diagnosis, pp. 229-233.

[12] Trigeol, J.-F, Bertin, Y, Lagonotte P 2006 Thermal modeling of an induction machine through the association of two numerical approaches. *IEEE Trans. Energy Convers*. pp 314–323.

[13] Ye L, Li D, Ma Y, Jiao B 2011 Design and performance of a water-cooled permanent magnet retarder for heavy vehicles. *IEEE Trans. Energy Convers*. pp 953–958.

[14] Chai F, Tang Y, Pei Y, Liang P, Gao H 2016 Temperature field accurate modeling and cooling performance evaluation of direct-drive outer-rotor air-cooling in-wheel motor. *Energies*.

[15] Mezani S, Takorabet N, Laporte B 2005 A combined electromagnetic and thermal analysis of induction motors. *IEEE Trans. Magn*, pp 1572–1575.

[16] Li Y, Wang X, Zhang J, Zhang L, Wu J.H 2019 Comparison and analysis of the arrangement of delta winglet pair vortex generators in a half coiled jacket for heat transfer enhancement, *International Journal of Heat and Mass Transfer*, pp 287-298.

[17] Asadi A, Pourfattah F 2019 Heat transfer performance of two oil-based nanofluids containing ZnO and MgO nanoparticles; a comparative experimental investigation, *Powder Technology*, pp 296-308,

[18] Hemmat Esfe M, Abbasian Arani AA 2018 An experimental determination and accurate prediction of dynamic viscosity of MWCNT(%40)-SiO2(%60)/5W50 nano-lubricant, *Journal of Molecular Liquids*, pp 227-237,

[19] Parsaiemehr M, Pourfattah F, Ali Akbari O, Toghraie D, Sheikhzadeh G 2018 Turbulent flow and heat transfer of Water/Al2O3 nanofluid inside a rectangular ribbed channel, *Physica E: Low-dimensional Systems and Nanostructures*, pp 73-84.

[20] Pourfattah F, Motamedian M, Sheikhzadeh G, Toghraie D, Ali Akbari O 2017 The numerical investigation of angle of attack of inclined rectangular rib on the turbulent heat transfer of Water-Al2O3 nanofluid in a tube, *International Journal of Mechanical Sciences*, pp 1106-1116.

[21] Raisia A, Aminossadati S.M, Ghasemi B 2016 An innovative nanofluid-based cooling using separated natural and forced convection in low Reynolds flows, *J Taiwan Inst Chem*.

[22] Akbari O.A, Toghraie D, Karimipour A 2015 Impact of ribs on flow parameters and laminar heat transfer of Water–aluminum oxide nanofluid with different nanoparticle volume fractions in a three-dimensional rectangular microchannel, *Adv. Mech. Eng*, pp 1–11.